J. exp. Biol. ***196****, 197–212 (1994)*
Printed in Great Britain © The Company of Biologists Limited 1994

‘ACTIVE’ SUGAR TRANSPORT IN EUKARYOTES

ERNEST M. WRIGHT, DONALD D. F. LOO,
MARIANA PANAYOTOVA-HEIERMANN, M. PILAR LOSTAO,
BRUCE H. HIRAYAMA, BRYAN MACKENZIE, KATHYRN BOORER
AND GUIDO ZAMPIGHI

Departments of Physiology and Anatomy and Cell Biology, UCLA School of Medicine, Los Angeles, CA 90024-1751, USA

Summary

Sugar transporters in prokaryotes and eukaryotes belong to a large family of membrane proteins containing 12 transmembrane alpha-helices. They are divided into two classes: one facilitative (uniporters) and the other concentrative (cotransporters or symporters). The concentrative transporters are energised by either H^+ or Na^+ gradients, which are generated and maintained by ion pumps. The facilitative and H^+-driven sugar transporters belong to a gene family with a distinctive secondary structure profile. The Na^+-driven transporters belong to a separate, small gene family with no homology at either the primary or secondary structural levels. It is likely that the Na^+- and H^+-driven sugar cotransporters share common transport mechanisms. To explore these mechanisms, we have expressed cloned eukaryote Na^+/sugar cotransporters (SGLT) in *Xenopus laevis* oocytes and measured the kinetics of sugar transport using two-electrode voltage-clamp techniques. For SGLT1, we have developed a six-state ordered model that accounts for the experimental data. To test the model we have carried out the following experiments. (i) We measured pre-steady-state kinetics of SGLT1 using voltage-jump techniques. In the absence of sugar, SGLT1 exhibits transient carrier currents that reflect voltage-dependent conformational changes of the protein. Time constants for the carrier currents give estimates of rate constants for the conformational changes, and the charge movements, integrals of the transient currents, give estimates of the number and valence of SGLT1 proteins in the plasma membrane. Ultrastructural studies have confirmed these estimates of SGLT1 density. (ii) We have perturbed the kinetics of the cotransporter by site-directed mutagenesis of selected residues. For example, we have identified a charged residue which dramatically changes the kinetics of charge transfer. (iii) We have examined the kinetics of sugar and Na^+ analogs. The V_{max} of sugar transport decreases dramatically with bulky phenyl glucosides and increases when H^+ replaces Na^+. These results permit us to extend and refine our model for transport. The model has been useful in the analysis of mutant SGLT1 proteins: in the case of a D176A mutant, the primary effect is to alter rates of conformational changes of the unloaded protein, and with the glucose/galactose malabsorption syndrome mutant D28N SGLT1, the mutation disrupts the delivery of SGLT1 glycosylated protein from the endoplasmic reticulum to the plasma membrane.

Key words: Na^+/glucose cotransporters, kinetics, freeze–fracture, presteady-state kinetics.

Introduction

In 1960 Bob Crane proposed that the 'active' transport of sugars was due to Na^+/sugar cotransport. Over the past 34 years the cotransport hypothesis has been confirmed, refined and extended to many other active transport systems in animals, plants and bacteria. These systems include the Na^+-driven amino acid, neurotransmitter, osmolyte and ion (e.g. PO_4^{3-}, I^- and SO_4^{2-}) systems in animals and the H^+-driven sugar and amino acid systems in bacteria and plants. It has even been extended to include the exchangers and antiporters, such as the Na^+/Ca^{2+} and Na^+/H^+ systems also found in cells from bacteria to man. Many of these transporters are major topics of this symposium. In this paper, we will limit our discussion to the Na^+/glucose cotransporter described by Crane for the intestinal brush-border membrane. We refer readers to Caspari *et al.* (1994) for a discussion of plant H^+/sugar cotransporters. About a decade ago, the intestinal Na^+/glucose cotransporter was finally identified as a 75 kDa protein and extrinsic fluorescent probes were employed to examine its conformational states (see Wright *et al.* 1994). Further biochemical work was impeded by the low abundance, lability and greasy nature of the cotransporter. However, a breakthrough was achieved in the field of membrane transporters in 1987 with the expression cloning of the intestinal Na^+/glucose cotransporter (SGLT1) in our laboratory using *Xenopus* oocytes (Hediger *et al.* 1987). This success was followed by the cloning and characterisation of a number of membrane carriers, channels and receptors using similar approaches. There are now over 350 papers in the literature using the oocyte expression system.

Structure

SGLT1 was the first member of a new gene family of transporters responsible for the 'active' transport of sugars, amino acids, vitamins and osmolytes in bacteria and animals. All are proteins containing 482–718 amino acid residues, and secondary structure analysis suggests that they consist of 12 transmembrane alpha-helices (Fig. 1). This motif is common to a large (more than 120 members) and diverse superfamily of transporters (see Henderson, 1993), but there is no homology between the SGLT1 family and these other transporters at the DNA, amino acid or secondary structural levels. SGLT1 is distinguished by the fairly large hydrophilic linkers between the membrane domains, the large hydrophilic link between transmembrane helices 11 and 12, the lack of a hydrophilic C terminus, and the presence of N-linked sugars between transmembrane helices 5 and 6. Glycosylation at this position suggests that both the N and C termini of the protein are on the cytosolic side of the membrane. Additional evidence of this topology of SGLT1 includes: (1) the exon/intron organisation of the gene (Turk *et al.* 1994); and (2) the identification of an external chymotrypsin cleavage site in the linker between transmembrane helices 11 and 12 (see Wright *et al.* 1994). Currently, a variety of experiments are in progress to test and refine this secondary structure model further as it is imperative to localise the transmembrane domains of the protein. A putative subunit of SGLT1 has been identified (Veyhl *et al.* 1993), but it should be noted that this protein is not obligatory for functional expression.

About 20 *SGLT1*-related clones have been isolated and sequenced (Table 1) and all have similar secondary structure profiles: 6–8 clones from different species appear to code for SGLT1 Na^+/glucose cotransporters (>84 % identity and >90 % similarity to SGLT1); another codes for a second Na^+/glucose cotransporter (76 % identity to SGLT1); two renal clones code for nucleoside and myoinositol cotransporters; and three code for bacterial proline and pantothenic acid cotransporters (25 % identity and 50 % similarity to SGLT1). There are at least nine other orphan clones with unknown function, and a few of these sequences are in the databases. Detailed alignment of the sequences of the functional SGLT1 clones shows that amino acids are conserved throughout all domains of the secondary structure and that the greatest differences are found in the C-terminal third of the proteins.

Differences in the amino acid sequences must account for the functional differences within this family, and this diversity offers an opportunity to locate residues and domains determining the function of these transporters. Finally, it should be noted that there is no homology between the SGLT1 family and other Na^+ cotransporters, such as those for neurotransmitters, bile salts and ions (e.g. PO_4^{3-} and SO_4^{2-}).

In common with the facilitated transporters with 12 transmembrane domains (Henderson, 1993), there is some evidence that the SGLT1 family evolved by gene duplication (Turk *et al.* 1994). There are a number of structural motifs duplicated in the exons coding for the N- and C-terminal halves of the protein. However, there is no significant homology between either half of SGLT1 and the transporters with 6–8 transmembrane domains, such as those for the bile acids and phosphate.

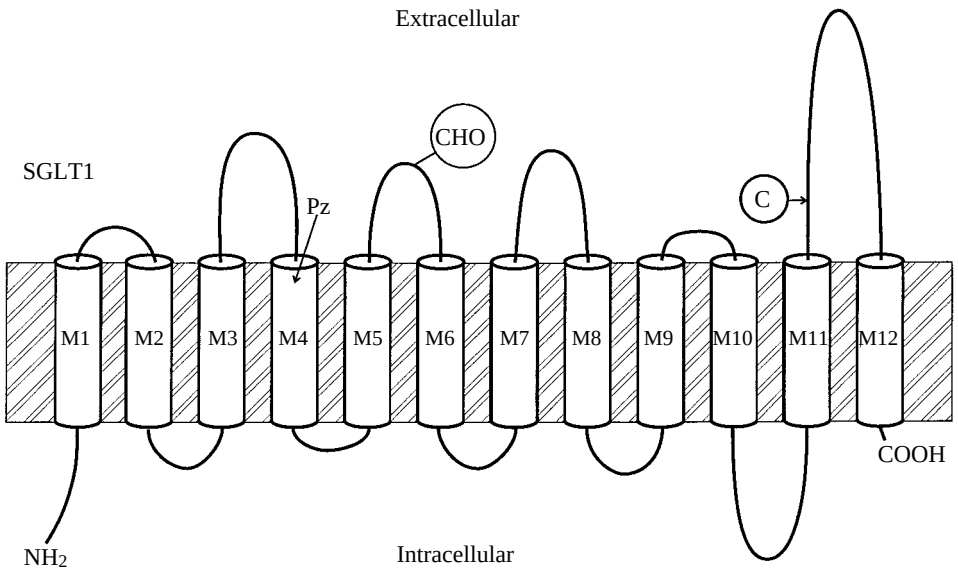

Fig. 1. A secondary structure model of SGLT1. The 662-residue membrane protein is shown to span the plasma membrane 12 times (M1–M12). The residue implicated in phlorizin binding (Pz at D176), the site of glycosylation (CHO at N248) and the extracellular chymotrypsin cleavage site (C) are indicated.

Table 1. *The Na^+ cotransport family: amino acid sequence comparisons of proteins homologous with the rabbit intestinal Na^+/glucose cotransporter*

Transporter	Abbreviation	Source	Identity (%)	Similarity (%)	Amino acids encoded
Na^+/glucose	SGLT1	Rabbit intestine	100	100	662
		Rabbit kidney	100	100	662
		Rat intestine	87	93	665
		Mouse intestine	86	93	665
		Human intestine	85	94	664
		LLC-PK_1 cells	84	92	662
Na^+/glucose	pSGLT2	LLC-PK_1 cells	76	89	664
Na^+/nucleoside	SNST1	Rabbit kidney	61	80	672
Na^+/myoinositol	SMIT1	Rabbit kidney	49	70	718
Hypothetical protein	Hypo	*Leishmania tarentolae*	26	58	443
Na^+/proline	Put P	*Escherichia coli*	26	55	502
		Salmonella typhimurium	25	56	502
Na^+/pantothenate	Pan F	*Escherichia coli*	22	53	482

The sequence comparisons are relative to the rabbit intestinal sequence.

Kinetics

SGLT1 is particularly well expressed in a functional form in oocytes and other heterologous expression systems. It is not unusual to find Na^+/glucose transport rates in cRNA-injected oocytes greater than 1000-fold higher than rates in control oocytes. This high expression level, together with electrical methods to measure transport, has encouraged us to conduct a comprehensive study of SGLT1 kinetics. In single oocytes, it is possible to measure both steady-state and pre-steady-state kinetic variables under a wide range of experimental conditions (see Parent *et al.* 1992*a*,*b*; Loo *et al.* 1993). The experimental design is illustrated by the experiment shown in Fig. 2. In this oocyte, a two-electrode voltage-clamp was used to hold the membrane potential at -100 mV and to record the membrane currents as a function of sugar and/or phlorizin composition of the extracellular Na^+ buffer. Addition of 5 mmol l^{-1} D-glucose produced an immediate 1 μA increase in the inward current, which was reversed by 100 μmol l^{-1} phlorizin, a competitive inhibitor of Na^+/glucose cotransport. In fact, phlorizin reduced the current below the baseline level, and even in the absence of sugar, phlorizin lowered the baseline current. Neither glucose nor phlorizin altered the current (<1 nA) in control oocytes. The phlorizin-sensitive glucose current and the phlorizin-sensitive current in the absence of sugar, the SGLT1 leak current, are well-documented properties of SGLT1.

We have measured the SGLT1 currents as a function of the external sugar, phlorizin and cation concentrations at voltages ranging from -150 to +50 mV, and the results have enabled us to propose a detailed model for Na^+/glucose cotransport (Parent *et al.* 1992*b*). The model, in cartoon form, and an equivalent kinetic scheme are presented in Fig. 3. In this six-state, ordered, non-rapid-equilibrium model, the free cotransporter protein C has

a valence of −2 and exists in two spatial conformations 1 ([C]′) and 6 ([C]″), where the ligand binding sites face the extra- or intracellular face of the membrane, respectively. Under physiological conditions, the membrane potential, −50 mV, favours 1 ([C]′), and the high external Na^+ concentration (100 mmol l^{-1}) promotes the binding of 2 Na^+ to form the neutral $[CNa_2]'$ complex 2. Since the intracellular fluid is sugar-free and contains a low Na^+ concentration (<20 mmol l^{-1}), more than 75 % of C exists as $[CNa_2]'$. Na^+ binding changes the conformation of [C]′ to allow sugar binding to form $[SCNa_2]'$ and then another conformational change occurs, state 3 to state 4, to present the ligands to the interior of the cell $[SCNa_2]''$. Sugar and Na^+ then dissociate and the final step is the return of the ligand-binding sites from the inner to the outer face of the membrane, state 6 ([C]″) to state 1 ([C]′). The complete reaction cycle results in the transport of 2 Na^+ and 1 sugar from the outside to the inside of the cell. A shunt pathway, state 2 ($[CNa_2]'$) to state 5 ($[CNa_2]''$), is shown for completeness, but under physiological conditions this pathway is fairly insignificant.

In Fig. 3B the individual rate constants are identified, k_{12}, k_{21}, k_{ij}, etc., and the voltage-sensitive steps are Na^+ binding and the [C]′ to [C]″ transitions. α', α'' and δ represent the fractions of the field felt by Na^+ binding and the [C]′ to [C]″ transitions and $\mu = FV/\boldsymbol{R}T$, where F is Faraday's constant, $\boldsymbol{R}$ is the gas constant and T is absolute temperature. Phlorizin, a competitive, non-transported inhibitor of SGLT1, binds to $[CNa_2]'$, state 2, to form the dead-end product $[PzCNa_2]'$.

The model accounts for the following experimental observations. (1) Sugar transport only occurs in the presence of Na^+. (2) Sugar transport is coupled to Na^+ transport with a

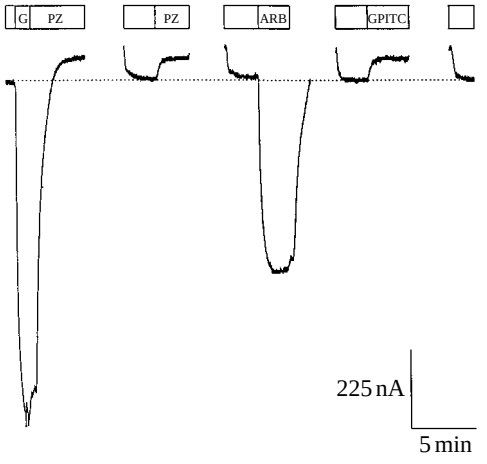

Fig. 2. Na^+/sugar currents recorded in an oocyte expressing SGLT1. A cRNA-injected oocyte was voltage-clamped at −100 mV in a Na^+ buffer solution, and currents were recorded in the presence and absence of 5 mmol l^{-1} sugar and/or 100 μmol l^{-1} phlorizin. After each test, the oocyte was washed in sugar- and Na^+-free buffer to return the currents to the baseline value (dotted line). G, D-glucose; PZ, phlorizin; ARB, arbutin; GPITC, glucosephenylisothiocyanate (1 mmol l^{-1}) (Lostao *et al.* 1994).

coupling coefficient of 2. This coupling is evident from the sugar depolarisation of the membrane potential, sugar stimulation of $^{22}Na^+$ uptake and Na^+ activation of sugar uptake with a Hill coefficient of close to 2. (3) The direction of sugar transport is reversed

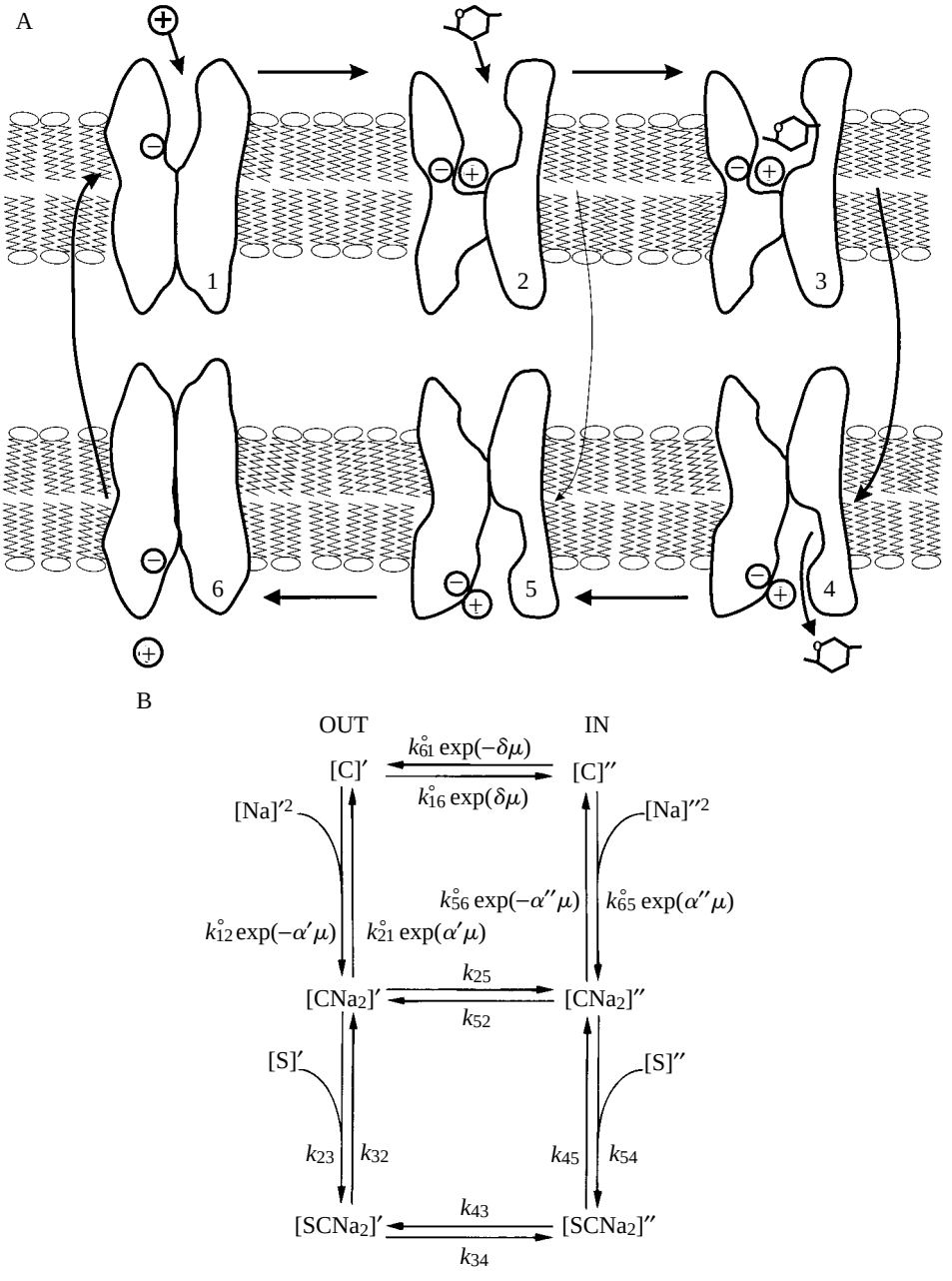

Fig. 3. The model for Na^+/glucose cotransport by SGLT1. (A) Cartoon. For clarity only one Na^+ is shown. (B) Equivalent kinetic scheme (see text). In B, state [C]′ is equivalent to state 1 in A, state [CNa_2]′ is equivalent to state 2 in A, etc.

if the Na^+ gradient is reversed. (4) There is a phlorizin-sensitive leak of Na^+ in the absence of sugar. (5) Increasing intracellular Na^+ concentration inhibits sugar uptake, *trans*-inhibition. (6) Sugar uptake is increased by negative membrane potentials.

Technical advances have enabled us to re-examine the model and to re-evaluate the 14 rate constants (Panayotova-Heiermann *et al.* 1994). The advance was the measurement of SGLT1 relaxation currents using a faster voltage-clamp with a settling time of less than 1 ms (Loo *et al.* 1993). Fig. 4 shows the rabbit SGLT1 relaxation currents using this new method. In the absence of sugar, transient SGLT1 currents are observed when the membrane potential is rapidly jumped from the holding potential, −100 mV, to new values ranging from −150 to +50 mV. For the three voltage steps shown, −50, −10 and +50 mV, large SGLT1 transients arise within milliseconds and then decay with time constants, τ, between 2 and 20 ms. Similar transients were also observed on returning the voltage to −100 mV (not shown). No SGLT1 transient currents were recorded in control oocytes. The time constants for the relaxation currents are voltage-dependent, Fig. 5A (open symbols), with a peak value of 18 ms at +10 mV. The integrals of the transient currents, charge transfer Q, are shown in Fig. 5C (open symbols), plotted against voltage. The Q/V curve is described by the Boltzmann relationship, where Q_{max} is the maximum charge transfer that can be observed, z is the valence of the moving charge and $V_{0.5}$ is the voltage where $0.5Q_{max}$ occurs. Q_{max} is proportional to the number of transporters expressed in the membrane, number=$Q_{max}ze_o$ (Loo *et al.* 1993), and values range up to 120 nC. This number is equivalent to 10^{12} transporters per oocyte assuming z=1, and a density of 40 000 μm^2 given the surface area of plasma membrane, 20×10^6 μm^2. This density approaches the highest

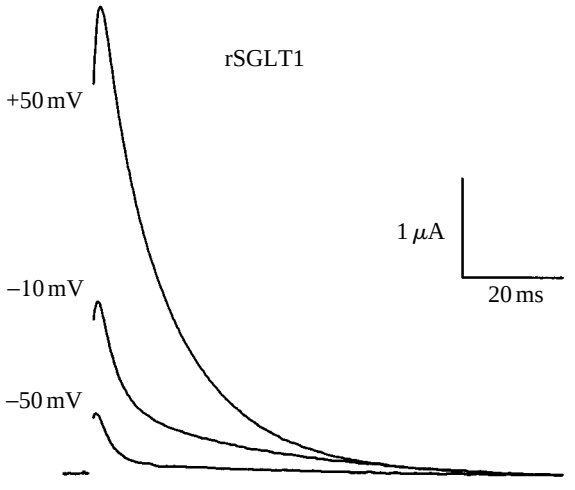

Fig. 4. Pre-steady-state current records for rabbit SGLT1 expressed in oocytes. The membrane potential was held at −100 mV and then stepped to various potentials V_t between −150 and +50 mV, and the membrane currents were recorded. The current traces for three voltages are shown. These SGLT1 currents were corrected for the oocyte capacitative currents. Note that each current rises to a peak and then decays to the baseline. On returning the membrane to the holding potential at −100 mV at the end of the 100 ms pulse, transient off-currents in the opposite direction were observed (not shown). The oocyte was bathed in NaCl buffer pH 7.4 with no sugar. Modified from Panayotova-Heiermann *et al.* (1994).

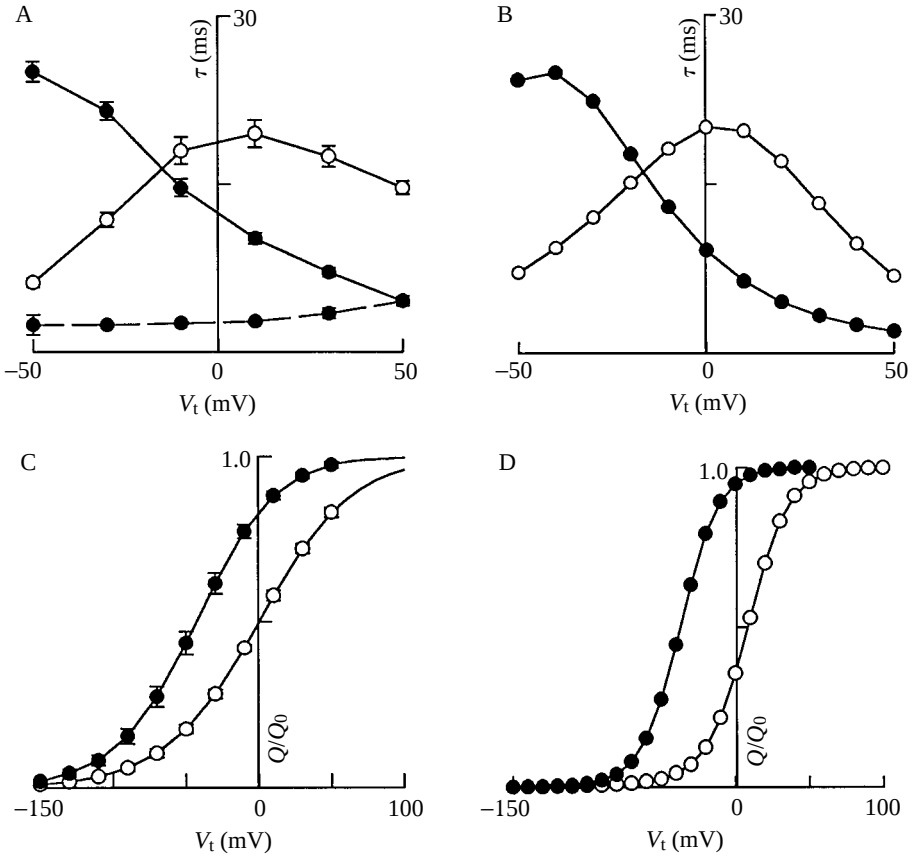

Fig. 5. Kinetics of charge transfer by SGLT1 expressed in oocytes. (A) The voltage-dependence of the relaxation time constant (τ) for wild-type (open circles) and D176A SGLT1 (filled circles, dashed line). The data shown are the mean of three SGLT1 and 10 D176A SGLT1 experiments. The time constants were obtained from the relaxation currents recorded at each voltage (see Fig. 4). The wild-type relaxation currents were fitted by a single time constant, while the mutant currents were fitted by two time constants. (B) The model predictions for A. (C) The voltage-dependence of SGLT1 charge transfer (Q). Q was obtained by integration of the current transients (see Fig. 4) and plotted against V_t. The curve was the fit of the data to the Boltzmann relationship: $Q = Q_{max}/[1 + \exp(V_t - V_{0.5})zF/\boldsymbol{RT}]$, where Q_{max} is the maximum charge transfer, z is the apparent valence of the charge, and $V_{0.5}$ is the voltage for $0.5Q_{max}$. For the wild type, these values were 80 nC, 1 and +0.5 mV, respectively, and for the D176A mutant 11 nC, 1 and −46 mV. (D) The simulated Q/V_t data. Open circles indicate the wild-type SGLT1 and filled circles the D176A SGLT1 mutant. All simulations were carried out by computer as described previously (Parent *et al*. 1992*b*; Loo *et al.* 1993). In the case of the wild-type SGLT1 (open symbols), these values were: α', 0.3; δ, 0.7; k_{16}, 100 s^{-1}, k_{61}, 35 s^{-1}; k_{12}, 20 000 $s^{-1}\,mol^{-2}$; k_{21}, 400 s^{-1}; k_{23}, 10^5 $s^{-1}\,mol^{-1}$; k_{32}, 20 s^{-1}; k_{34}=k_{43}, 50 s^{-1}; k_{45}, 800 s^{-1}; k_{54}, 2.24×10^8 $s^{-1}\,mol^{-1}$; k_{56}, 16 s^{-1}; k_{65}, 50 $s^{-1}\,mol^{-2}$, k_{25}, 0.01 s^{-1}; and k_{52}, 0.56 s^{-1}. Simply changing k_{16} and k_{61} to 800 and 8 s^{-1} simulates the pre-steady-state and steady-state kinetics observed for the mutant (see also Fig. 7). Modified from Panayotova-Heiermann *et al.* (1994).

known for any plasma membrane protein. Independent verification of the number of cotransporters expressed in oocyte membranes was obtained by freeze–fracture electron microscopy (Zampighi *et al.* unpublished results). A replica of the P face, the cytoplasmic

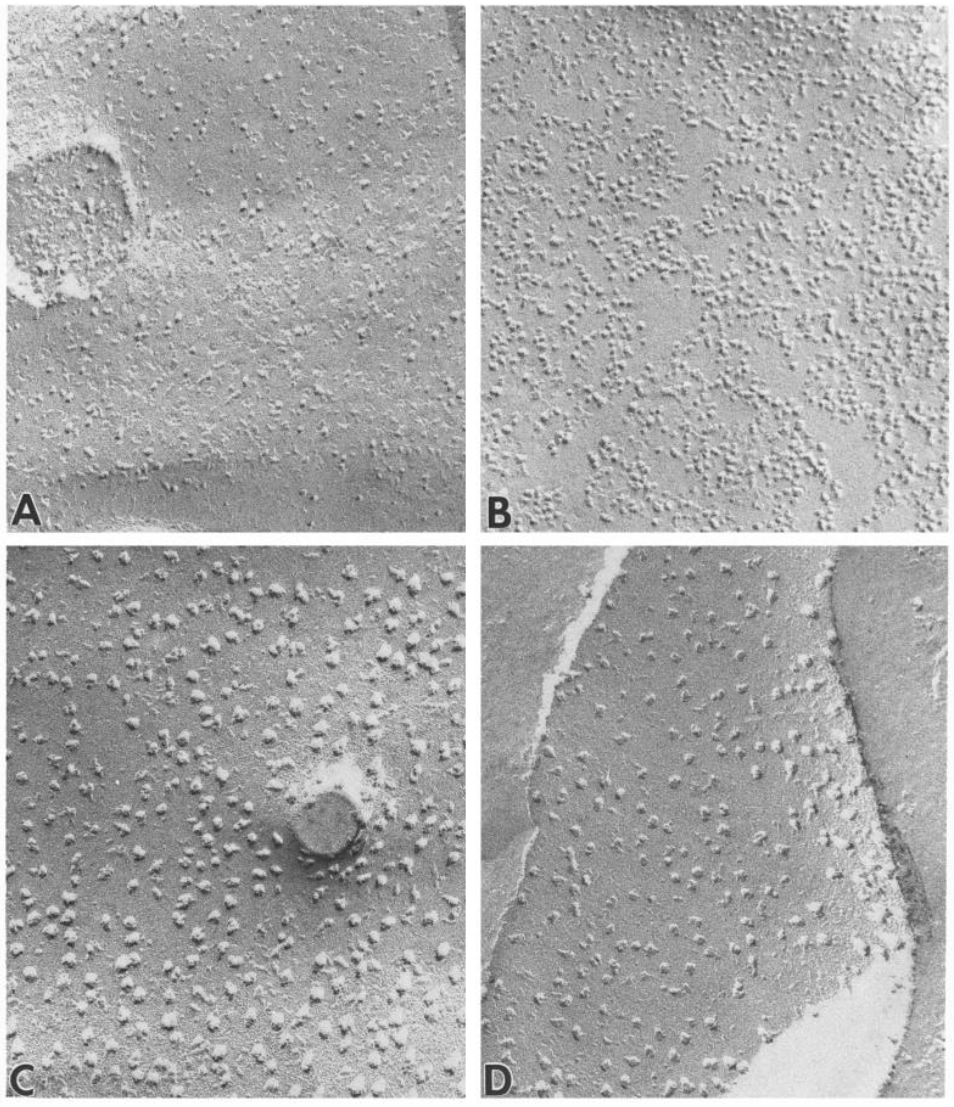

Fig. 6. Freeze-fracture replicas of plasma membranes from oocytes injected with water (A and C) and with SGLT1 cRNA (B and D). A and B show the P face and C and D show the E face. Note the cross sections of microvilli seen in A and C. In control oocytes, the intramembrane particles (IMPs) were found on the E face; the P face shows pits and many fewer IMPs. In the membranes from the SGLT1-cRNA-injected oocytes, there was no change in the density of the E face IMPs, but numerous new IMPs were inserted into the P face. In this experiment, where there was relatively low expression of the Na^+/glucose transporter in the oocyte, the density of the P face IMPs increased from about 200 to 2000 μm^{-2}. Total magnification 100 000×. Modified from Zampighi *et al.* (unpublished results).

leaflet, of the plasma membrane obtained from a SGLT1-cRNA-injected oocyte is presented in Fig. 6 along with a replica from a control oocyte. Very few intramembrane particles, IMPs, are observed in the P face of control oocytes, but a high density of 7–8 nm diameter IMPs was observed in the oocyte expressing SGLT1.

There was a direct correlation between the density of these IMPs and Q_{max}, and in oocytes injected with cRNA coding for a mutant protein, D28N SGLT1, there was no sugar transport, charge transfer or an increase in IMP density above background. The highest density of individual IMPs that we could resolve was about 5000 μm^{-2} in oocytes with a Q_{max} of 30 nC; at greater levels of expression it was not possible to resolve individual IMPs. We conclude that the IMPs observed in the P face of plasma membranes containing functional cotransporters are, in fact, the cotransporter protein and that Q_{max} is a valid measure of the number of cotransporters expressed in the membrane. With regard to the model, this result removes an assumption about the number of transporters in the membrane.

What is SGLT1 charge transfer? Our interpretation is that charge transfer across the membrane reflects voltage-dependent conformational changes of the transport protein. In the absence of sugar at a holding potential of −100 mV, most of SGLT1 is in the Na^+-bound form with active sites facing the external solution, state 2 ($[CNa_2]'$) in Fig. 3. Stepping the potential to +50 mV then causes Na^+ to dissociate and the negatively charged protein to reorientate in the membrane field to state 6 ($[C]''$). About 30 % of the charge movement is due to Na^+ dissociation and about 70 % to protein reorientation. Returning the potential to −100 mV results in a complete reversal of the charge movement. The time constants for the charge transfer therefore provide rich information about the rate constants for the conformation changes, k_{21}, k_{12}, k_{16} and k_{61}. The experimental and simulated τ/V and Q/V curves for the wild-type SGLT1 transporter are shown in Fig. 5; note the excellent agreement between the data (Figs 5A,C) and the simulations (Figs 5B,D). The model actually predicts two time constants for the charge transfer, but one is below the resolution of the two-electrode voltage-clamp. However, we have been able to record two time constants for both the on- and the off-pulses using the cut-open oocyte preparation (Loo *et al.* 1994). The fast time constants are in the sub-millisecond range and they will provide another test of our model.

Selected examples of steady-state kinetics variables and their simulation for wild-type SGLT1 (open symbols) are included in Fig. 7. The apparent affinities for sugar and Na^+ as a function of membrane potential at saturating Na^+ and sugar concentrations, respectively, are shown. The apparent K_m for sugar was about 0.175 mmol l^{-1} and it was independent of potential between −50 and −150 mV in both the experiment and the simulation. The apparent K_m for Na^+ varied between 14 and 8 mmol l^{-1} between −30 and −150 mV in both experiment and simulation. Therefore, one set of rate constants can reproduce both the pre-steady-state and steady-state kinetics of SGLT1. The higher resolution relaxation methods only required minor changes in the original set of rate constants (Parent *et al.* 1992*b*), i.e. an increase in both k_{16} and k_{61} by a factor of 3–5.

Model testing

Our model has proved useful in designing experiments and in the interpretation of results. We have designed experiments to probe rate-limiting steps and have used the model to explain the effect of mutations on sugar transport. This use will be illustrated by three examples taken from recent work: (1) a study of one SGLT1 mutation that dramatically alters charge transfer (Panayotova-Heiermann *et al.* 1994); (2) the kinetics of phenylglucoside transport (Lostao *et al.* 1994); and (3) the kinetics of H^+/sugar cotransport (Hirayama *et al.* 1994).

Mutations and charge transfer

In a continuing search for residues in the membrane domain of SGLT1 that play a role in the kinetics of charge transfer, we changed aspartic acid 176 in putative transmembrane helix 4 to a neutral residue, D176A. This mutation altered the kinetics of charge transfer (Fig. 5, filled symbols). Both the τ/V and Q/V curves were shifted by about 60 mV to more negative values, but there was no change in the apparent valence, z. In order to simulate the data, it was necessary to change the rate constants, k_{16} and k_{61}, for

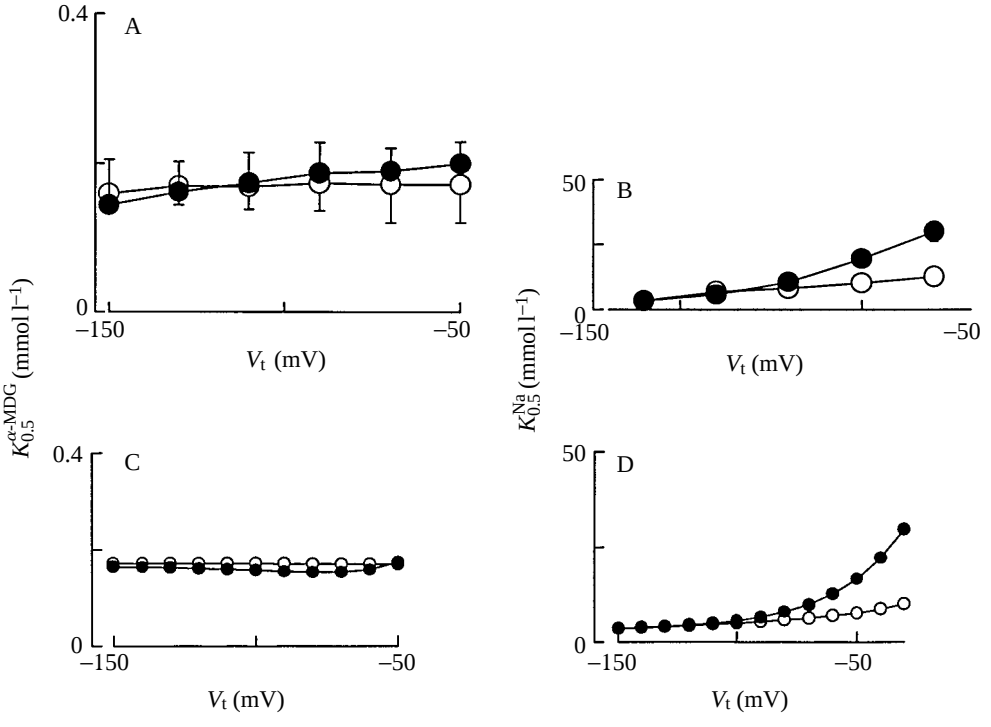

Fig. 7. Sugar and Na^+ apparent affinities for wild-type and D176A SGLT1 expressed in oocytes. A and C show the measured and simulated $K_{0.5}$ values for α-MDG at 100 mmol l^{-1} NaCl as a function of membrane potential, and B and D show the measured and simulated values for $K_{0.5}$ values for Na^+ at 5 mmol l^{-1} α-MDG as a function of membrane potential. Open symbols are for wild type and filled symbols are for the mutant. Modified from Panayotova-Heiermann *et al.* (1994). Values in A are mean ± S.E.M., N=3.

the reorientation of SGLT1 in the membrane to account for the change in $V_{0.5}$ and the relaxation time constants (Fig. 5B,D). Essentially, this mutation alters the distribution of SGLT1 between states 1 and 6; at physiological membrane potentials in the absence of sugar and Na^+, a higher fraction of SGLT faces inward than in the wild type. No alteration in charge transfer kinetics occurs when D176 is replaced by N176, indicating that very polar residues at position 176 maintain the preferred conformation by electrostatic interactions with another residue. The preferred conformation is also the most stable conformation as Q_{max} for D176A SGLT1 is only about 14% of the control value, implying that D176 is in the membrane domain. The loss of electrostatic interactions in the hydrophobic core of the protein in D176A SGLT1 would be energetically unfavourable.

Given that D176A exhibits markedly altered charge transfer kinetics that can be accounted for by changes in the rate constants for reorientation of the unloaded transporter in the membrane, how does this effect sugar transport? The apparent affinity for sugar is unaffected (Fig. 7A, filled symbols), while there is a slight decrease in the apparent affinity of Na^+ at potentials of -50 mV or lower (Fig. 7B, filled symbols). The slight change in apparent Na^+ affinity is also reflected in a slight shift in the shape of the SGLT1 *I*/*V* curve at low voltages (not shown). As expected from the decrease in Q_{max} to 14% of the control value, there was a proportional decrease in the rate of sugar transport. Note the very good agreement between the experimental and simulated kinetic variables: compare Fig. 7A and C and Fig. 7B and D.

We conclude from these studies that the model can account for the kinetics of the D176A mutant with a change in the rate constants for a partial step in the reaction cycle, i.e. the conformational changes of the unloaded carrier.

Kinetics of phenylglucoside transport

It is well documented that glucosides are transported by the Na^+/glucose cotransport (Landau *et al.* 1962). Substrates accepted include α-methyl-glucoside and arbutin (4-hydroxphenyl-β-D-glucopyranoside). We reasoned that it would be informative to study the transport kinetics of bulky glucopyranosides using the oocyte expression system (Lostao *et al*. 1994). Fig. 2 shows that arbutin is transported by SGLT1: it produces an inward current about 60% of that for D-glucose. The apparent K_m for arbutin was about 1 mmol l^{-1} but, unlike the monosaccharides, the maximal rate of transport was only 80% of that for α-methyl-D-glucopyranoside (α-MDG). The V_{max} values for other phenylglucosides were even lower, e.g. for phenyl-β-D-glucopyranoside and helicin (salicil-aldehyde-β-D-glucopyranoside) the V_{max} values were only 50 and 25% of the α-MDG value at -150 mV. The α-phenyl derivatives are not transported.

The lower V_{max} values for the bulky sugar analogues could be due to an impairment of the transport step across the membrane, i.e. to the isomerisation of the fully loaded carrier in the membrane ($[SNa_2C]'$ to $[SNa_2C]''$). In fact, a reduction in the rate constant from 50 to 25, 12 and 5 s^{-1} can account for the V_{max} values for arbutin, phenylglucose and helicin respectively. The transport of phenylglucosides by SGLT1 also has an important bearing on the conformational changes of the protein responsible for transport in that the protein

has to accommodate molecules as large as 1 nm×0.5 nm×0.5 nm. This result is similar to oligosaccharide transport by lactose permease mutants (Olsen and Brooker, 1993).

Not all β-phenylglucosides are transported by SGLT1. As shown in Fig. 2, simply substituting an -NCS group for -OH on the phenyl ring of arbutin converts the molecule from a substrate into an inhibitor. β-D-glucopyranosyl-phenylisothiocyanate (GPITC) behaves like phlorizin in inhibiting the leak current with an inhibitor constant of less than 0.5 mmol l^{-1}. Since GPITC can also irreversibly block transport in rabbit brush-border membrane vesicles, and since inhibition is protected by Na^+ and glucose, it is reasonable to conclude that GPITC is covalently labelling a lysine residue some 0.8 nm away from the sugar binding pocket. This lysine residue may be the one previously identified as being near the glucose binding site (see Wright *et al.* 1994).

Phlorizin (phloretin-2-β-D-glucopyranoside) is the most potent inhibitor of Na^+/glucose cotransport with a K_i of 5–10 μmol l^{-1}. This high potency is in part due to interactions of the para-OH group on the β-phenyl ring with the cotransporter protein. One candidate residue in the protein must be D176, because the phlorizin K_i increased by four- to sixfold when this residue was replaced with alanine (Panayotova-Heiermann *et al.* 1994). If this is the case, then D176 is some 1 nm from the sugar binding pocket. On aggregate, these results suggest a vestibule leading to the external sugar binding pocket of SGLT1, and that both non-specific (hydrophobic) and specific (electrostatic) interactions occur between the residues lining the vestibule and that the phenylglucosides determine access and transport. Identification of the residues in both the sugar binding site and the vestibule is needed to unravel the molecular architecture of the active site.

Kinetics of H^+/glucose cotransport by SGLT1

According to our model, the rate-limiting step for transport at high negative membrane potentials, −150 mV, is the dissociation of Na^+ from the internal binding site, i.e. $[CNa_2]''$ to $[C]'' + 2Na^+$ (Parent *et al.* 1992*b*). One way to test this prediction is to replace Na^+ with other cations and measure transport kinetics. Since Hoshi *et al.* (1986) reported that pH gradients could drive sugar transport, we (Hirayama *et al*. 1994) decided to examine the kinetics of H^+/sugar transport by SGLT1. Fig. 8 shows one experiment where, in the complete absence of Na^+, a pH gradient of 2 units was sufficient to generate a phlorizin-sensitive sugar current and a phlorizin-sensitive leak current. In this oocyte, the H^+/sugar current was about 30 % of the Na^+/glucose current at pH 7.5. There was no sugar transport at pH 7.5 in the absence of Na^+, and the currents at an external pH of 5.5 were independent of the cation used to replace Na^+. There were no currents in control oocytes at pH 5.5. These results confirm H^+/glucose cotransport by SGLT1.

The steady-state kinetics of H^+/glucose cotransport were then determined. The apparent affinity for α-MDG was 18 mmol l^{-1} at −50 mV and pH 5.5, whereas it was 0.2 mmol l^{-1} in 100 mmol l^{-1} NaCl at −50 mV and pH 7.5. In contrast, the V_{max} was 150% of that in the presence of Na^+. Sugar currents were then measured in Na^+-free solutions from pH 7.5 to 5.5. The H^+ activation curves gave a Hill coefficient of 1.5 and an apparent affinity for H^+ of 1–2 μmol l^{-1} at −50 mV. These results indicate a coupling coefficient of 2 and that the affinity of SGLT1 for H^+ is about 1000 times higher than that for Na^+, but the apparent affinity of the H^+-loaded protein for sugar was about 100 times lower than that of the Na^+-

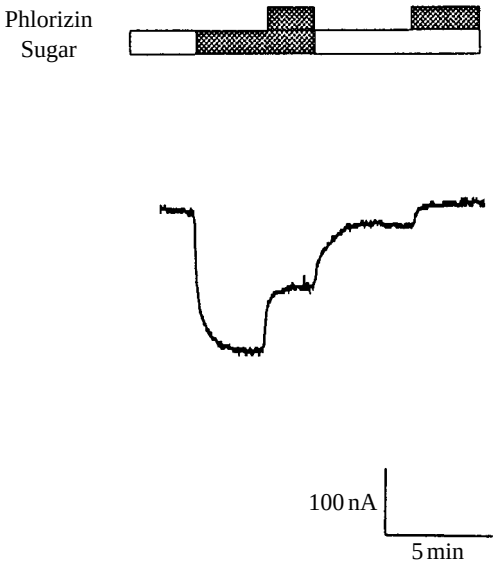

Fig. 8. SGLT1 currents in the presence of H^+. In this cRNA-injected oocyte, the membrane was clamped at -50 mV and the current was recorded while varying the bathing solution. The oocyte was bathed in 100 mmol l^{-1} choline chloride at pH 5.5 and α-MDG and phlorizin were added at the times indicated. 5 mmol l^{-1} sugar produced an inward current of 220 nA, and this was partially inhibited by adding 10 μmol l^{-1} phlorizin. After washing out the sugar and phlorizin, 10 μmol l^{-1} phlorizin inhibited the baseline current in the absence of sugar, i.e. the SGLT1 H^+ leak current. Modified from Hirayama *et al.* 1994).

loaded protein. In other words, the conformation of the H^+ form of SGLT1 was not optimal for sugar binding. Nevertheless, the V_{max} for H^+/sugar that transport was greater than that for Na^+/sugar transport. This finding suggests that the magnitude of the rate-limiting step is changed in the presence of protons, and this is consistent with this step being the internal dissociation of cations from SGLT1. Similar observations have been made for the bacterial melibiose transporter, in which both Na^+ and H^+ can drive transport (Bassilana *et al.* 1987; Damiano-Forano *et al.* 1986). The affinity of the protein for H^+ was 1000 times greater than for Na^+, but the apparent affinity for sugar was 50 times higher in the presence of Na^+ than in the presence of H^+. However, the V_{max} was much greater for H^+/melibiose than for Na^+/melibiose. For both the mammalian glucose and the bacterial melibiose transporters, it appears that the ligand bound determines the sugar affinity and the rate of the limiting step, cation dissociation from the internal site. This result suggests that the two transporters share a common transport mechanism even though there is no homology between the bacterial and mammalian proteins at the amino acid level.

Conclusions

The Na^+/glucose cotransporter SGLT1 has proved to be an excellent model system in which to study cotransporter mechanisms when expressed in *Xenopus* oocytes. Electrophysiological methods, both steady-state and pre-steady-state, have provided

unique insights into the partial reactions of the transport cycle. We are rapidly reaching the stage where it is possible to study transport as a function of intracellular ligands using the cut-open oocyte preparation, and this approach promises to remove uncertainty about the kinetics of the internal binding reactions and sugar efflux. One assumption in our model that needs to be critically tested is that either the two sodium binding sites of SGLT1 are identical or that the binding of 1 Na^+ is rate-limiting (Parent *et al.* 1992*b*). This assumption simplified the model to a six-state system with 14 rate constants. Preliminary experiments have detected some heterogeneity of Na^+ binding to SGLT1, but further work is required to resolve this question. Important clues may emerge from a detailed kinetic analysis of SGLT2, a Na^+/glucose cotransporter with one Na^+ binding site (Mackenzie *et al.* 1994).

Our experiments with SGLT1 also show the power of electrophysiological methods to unravel the effect of mutations on transport. As illustrated with the D176A SGLT1 mutant, it is possible, with a combination of pre-steady-state and steady-state experiments, to determine the amount of transporter in the plasma membrane and to pinpoint the partial reaction step affected by the mutation–ligand binding, conformational changes, etc. In the case of the D28N SGLT1 mutation causing glucose/galactose malabsorption (GGM) in one family (Turk *et al.* 1991), a combination of biochemical and biophysical techniques indicates that the defect appears to be in the transport of core glycosylated SGLT1 protein from the endoplasmic reticulum to the plasma membrane: the mutant SGLT1 RNA is translated, the protein is inserted into the endoplasmic reticulum and glycosylated, but it does not reach the plasma membrane as judged by charge measurements and freeze–fracture electron microscopy. We have identified 14 other missense mutations in GGM patients (M. Martin, E. Turk and E. M. Wright, unpublished results), and we anticipate that these experimental approaches will establish how these new mutations cause the malabsorption syndrome.

These studies were supported by grants from the NIH (DK 19567; DK 44602 and NS 25554).

References

BASSILANA, M., POURCHER, T. AND LEBLANC, G. (1987). Facilitated diffusion properties of Melibiose permease in *Escherichia coli* membrane vesicles. *J. biol. Chem.* **262**, 16865–16870.

CASPARI, T., WILL, A., OPERAKOVA, M., SAUER, N AND TANNER, W. (1994). Hexose/H^+ symporters in lower and higher plants. *J. exp. Biol.* **196**, 483–491.

DAMIANO-FORNAO, E., BASSILANA, N. AND LEBLANC, G. (1986). Sugar binding properties of the melibiose permease in *Escherichia coli* membrane vesicles. *J. biol. Chem.* **261**, 6893–6899.

HEDIGER, M. A., COADY, M. J. AND IKEDA, T. S. (1987). Expression cloning and cDNA sequencing of the Na^+/glucose co-transporter. *Nature* **330**, 379–381.

HENDERSON, P. J. (1993). *Current Opinion Cell Biol.* **5**, 708–721.

HIRAYAMA, B. A., LOO, D. D. F. AND WRIGHT, E. M. (1994). Protons drive sugar transport through the Na^+/glucose cotransporter (SGLT1). *J. biol. Chem.* **269** (in press).

HOSHI, T., TAKUWA, N., ABE, M. AND TAJIMA, A. (1986). Hydrogen-coupled transport of D-glucose by phlorizin-sensitive sugar carrier in intestinal brush border membranes. *Biochim. biophys. Acta* **861**, 482–488.

LANDAU, B. R., BERNSTEIN, L. AND WILSON, T. H. (1962). Hexose transport by hamster intestine *in vitro*. *Am. J. Physiol.* **203**, 237–240.

LOO, D. D. F., BEZANILLA, F. AND WRIGHT, E. M. (1994). Two voltage-dependent steps are involved in the partial reactions of the Na^+/glucose cotransporter (SGLT1). *FASEB J.* **8**, A1993.

LOO, D. D. F., HAZAMA, A., SUPPLISSON, S., TURK, E. AND WRIGHT, E. M. (1993). Relaxation kinetics of the Na^+/glucose cotransporter. *Proc. natn. Acad. Sci. U.S.A.* **90**, 5767–5771.

LOSTAO, M. P., HIROYAMA, B. A., LOO, D. D. F. AND WRIGHT, E. M. (1994). Phenyl glucosides and the Na^+/glucose cotransporter (SGLT1): analysis of interactions. *J. Membr. Biol.* **142** (in press).

MACKENZIE, B., PANAYOTOVA-HEIERMANN, M., LOO, D. D. F., LEVER, J. E. AND WRIGHT, E. M. (1994). SAAT1 is a low affinity Na^+/glucose cotransporter and not an amino acid transporter. *J. biol. Chem.* **269** (in press).

OLSEN, S. G. AND BROOKER, R. J. (1993). Lactose permease mutants which transport (malto-) oligosaccharides. *J. Bacteriol.* **175**, 6269–6275.

PANAYOTOVA-HEIERMANN, M., LOO, D. D. F., LOSTAO, P. M. AND WRIGHT, E. M. (1994). Sodium–D-glucose cotransporter charge movements involve polar residues. *J. biol. Chem.* (in press).

PARENT, L., SUPPLISSON, S., LOO, D. D. F. AND WRIGHT, E. M. (1992*a*). Electrogenic properties of the cloned Na^+/glucose cotransporter. I. Voltage-clamp studies. *J. Membr. Biol.* **125**, 49–62.

PARENT, L., SUPPLISSON, S., LOO, D. D. F. AND WRIGHT, E. M. (1992*b*). Electrogenic properties of the cloned Na^+/glucose cotransporter. II. A transport model under nonrapid equilibrium conditions. *J. Membr. Biol.* **125**, 63–79.

TURK, E., MARTIN, M. AND WRIGHT, E. M. (1994). Structure of the human Na^+/glucose cotransporter gene SGLT1. *J. biol. Chem.* (in press).

TURK, E., ZABEL, B., MUNDLOS, S., DYER, J. AND WRIGHT, E. M. (1991). Glucose/galctose malabsorption caused by a defect in the Na^+/glucose cotransporter *Nature* **350**, 354–356.

VEYHL, M., SPANGENBERG, J., PUSCHEL, B., POPPE, R., DEKEL, C., FRITZSCH, G., HAASE, W. AND KOEPSELL, H. (1993). Cloning of a membrane-associated protein which modified activity and properties of the Na^+–D-glucose cotransporter. *J. biol. Chem.* **268**, 25041–25053.

WRIGHT, E. M., HIRAYAMA, B. A., LOO, D. D. F., TURK, E. AND HAGER, K. (1994). Intestinal sugar transport. In *Physiology of the Gastrointestinal Tract*, 3rd edition, vol. II (ed. L. R. Johnson), pp. 1751–1772. New York: Raven Press.